

## Magnetoresistance of an entangled single-wall carbon-nanotube network

G. T. Kim, E. S. Choi, D. C. Kim, D. S. Suh, and Y. W. Park\*

*Department of Physics and Condensed Matter Research Institute, Seoul National University, Seoul 151-742, Korea*

K. Liu, G. Duesberg, and S. Roth

*Max-Planck Institut für Festkörperforschung, Heisenbergstraße 1, D-70569 Stuttgart, Germany*

(Received 22 April 1998)

The resistivity  $\rho(T)$  and magnetoresistance (MR) ( $\Delta\rho/\rho$ ) of an entangled single-wall carbon-nanotube network are investigated. The temperature dependence of the resistivity shows a negative  $d\rho/dT$  from  $T = 4.3\text{--}300$  K with no resistivity minimum, which is fitted well to the two-dimensional variable-range-hopping (VRH) ( $\rho(T) = \rho_0 \exp[(T_0/T)^{1/3}]$ ) formula with  $T_0 = 259.2$  K. The MR shows a negative  $H^2$  behavior at low magnetic field. At  $T \leq 3.8$  K and high magnetic field, the negative MR becomes positive. The positive MR tends to be saturated for  $H > 10$  T. The negative MR with a positive upturn can be decomposed into a positive contribution from the two-dimensional spin-dependent VRH and a negative contribution from the two-dimensional weak localization, with some contribution of the Ni impurities in the sample found with the transmission electron microscope and by energy dispersive spectrometer analysis. [S0163-1829(98)07848-5]

### I. INTRODUCTION

Since Iijima<sup>1</sup> discovered the carbon nanotube, many theoretical and experimental works have been done on this noble structure.<sup>2–29</sup> The geometric structure of a carbon nanotube is known to determine the electronic structures of metals, semimetals, and semiconductors, depending on their diameter, number of concentric shells, and chirality.<sup>2</sup> Among the various kinds of carbon nanotubes, the single-wall carbon nanotube (SWCN) is the most simplified structure, and especially the (10,10) structure is believed to be metallic.<sup>13,17,24,26</sup> The temperature dependence of the susceptibility<sup>4–6</sup> shows the Pauli paramagnetic susceptibility of conduction electrons at high temperature, and the gyromagnetic ratio in the electron-spin resonance<sup>11</sup> was reported to be 2.0022, close to that of the free electron. Thermoelectric power measurement also shows a metallic temperature dependence without any gap opening at low temperature.<sup>23</sup> However, the resistivity increases upon cooling for most of the carbon nanotube samples. Recently, Fischer *et al.*<sup>17</sup> reported the metallic linear temperature dependence of the resistivity for the SWCN. The resistivity decreases approximately 5% from room temperature down to  $T = 35$  K, and then increases for  $T < 35$  K.

At extremely low temperatures, Langer and co-workers<sup>3,10</sup> reported an abnormal temperature dependence of the resistivity, showing two resistance maxima with a saturation behavior of  $T \rightarrow 0$ . The temperature dependence of the resistivity changes very sensitively with different samples depending on the preparation methods such as the heat treatment.<sup>23,24,26</sup> To understand the absence of metallic resistivity at low temperature, the authors of Ref. 20 proposed a heterogeneous model composed of energy barriers and metallic islands. Recent studies by scanning tunneling spectroscopy<sup>28,29</sup> showed the existence of various energy gaps in the SWCN of different chirality on the surface of the bundle, and, even in the same tube, various energy gaps were found depending on the position. These may correspond to

the energy barriers in the heterogenous model. In the localization picture, structural defects and impurities might cause weak or strong localizations depending on the degree of disorder. There were many reports based on the weak-localization (WL) picture, suggesting that the conduction is mainly that of a two-dimensional conductor at low temperature.<sup>7,12</sup> Lee, Kim and Tamanek<sup>27</sup> argued theoretically about the role of nickel particles in forming the SWCN. The Ni catalyst is essential for synthesis of SWCN. The existence of Ni impurities in the SWCN can lead to an argument similar to the Kondo effect, because of their magnetic properties. In fact, the susceptibility data of a carbon nanotube show a Curie-type contribution of the localized moment larger than that of conduction electron itself at low temperature,<sup>4–6</sup> even after a cautious heat treatment to remove the transition metal impurities. Kosaka *et al.*<sup>11</sup> reported the double electron-spin-resonance (ESR) lines composed of the conduction electron and the localized moment, and the change of the ESR line of a localized moment, by annealing the sample at high temperature, indicating the existence of a magnetic moment of the impurities. Therefore, we can infer that there remain some transition-metal impurities even after the cautious purification. It is not clear how large the effect of transition-metal impurities is in the low-dimensional conductor, but we were first motivated by the existence of the Ni impurities.<sup>31–40</sup> We have attempted quantitative analysis of the temperature dependence of the zero-field resistivity as well as the magnetoresistance (MR) with the localization pictures,<sup>9,10,12,41–46</sup> with an additional contribution from the magnetic impurity Ni. The results are rather consistent with the two-dimensional variable-range-hopping (VRH) model, with the two-dimensional WL under a magnetic field. The Kondo-effect-like analysis indicates that the magnetic impurity Ni may also play a significant role in the observed MR.

### II. EXPERIMENTS

SWCN's were synthesized by the arc-plasma method in the presence of a Ni-Y catalyst.<sup>19</sup> Mats of entangled

SWCN's were obtained. These mats were cut into rectangular bars,  $2 \times 1 \times 0.1 \text{ mm}^3$  in size. Platinum wire pressure contacts were applied in a four-probe configuration. The temperature dependence of the resistivity between  $T=4.3$  and 300 K was measured by an Oxford variable temperature cryogenic system equipped with a 12-T superconducting magnet. Two EG&G 5210 Lockin Amplifiers with a reference frequency  $f_r=13.7 \text{ Hz}$  were used for the measurement. We measured the MR by sweeping the magnetic field slowly to avoid electromotive induction and self-heating. The current we applied was  $1 \mu\text{A}$ . To obtain a stable temperature in MR measurement, we waited a reasonable amount of time while monitoring the zero-field resistance after setting the optimum helium vapor pressure for the temperature control. After the temperature became stable, we applied the magnetic field. To confirm the stability of the temperature, we checked the zero-field resistance again after the magnetic-field sweeping. At high temperature,  $T=225 \text{ K}$ , we controlled the heating power applied to the sample holder to stabilize the temperature. To characterize the SWCN sample, some mats were sonicated in the presence of a sodium dodecylsulfate in an aqueous environment.<sup>21</sup> The suspension was deposited on silicon oxide substrate and investigated by scanning force microscopy. These studies revealed typical tube sizes of  $1.2 \mu\text{m}$  in length and  $1.1 \text{ nm}$  in height.<sup>22</sup> Thick objects were interpreted as ropes, not completely decomposed into individual tubes during sonication. From these studies, we concluded that our sample was an entangled network, predominantly of ropes of SWCN's.

### III. RESULTS AND DISCUSSION

The transmission electron microscope picture of the SWCN network sample is shown in Fig. 1. The finest tubes of diameter  $\approx 1.5 \text{ nm}$  shown in Fig. 1 can be identified as the SWCN's. One may notice that the majority of the tubes are in bundle forms whose diameters are larger than  $5 \text{ nm}$ . This indicates that the individual SWCN's form the ropes where the intertubular interaction could be significant.<sup>24,25</sup> In addition, dark spots are observed near the stem of the bundles. Independently, energy dispersive spectrometer (EDS) data for the sample show clear peaks identified as Ni impurities, as in the inset of Fig. 1. The Ni impurities could originate from the catalyst in synthesizing the SWCN, and are located in the dark-spots area, forming a mixture with carbon particles.

The MR's are plotted in Fig. 2 for different temperatures. The overall MR's are negative, similar to what was found by others.<sup>7,8,18</sup> At  $T=1.5, 2.33, 2.92, 3.8,$  and  $6.7 \text{ K}$ , the MR's show upturns toward positive values. In the case of  $T=1.5 \text{ K}$ , there is a reduction of positive slope which may indicate the saturation for  $H > 10 \text{ T}$ . The negative minimum of the MR moves to a higher field as temperature rises. At  $T=225 \text{ K}$ , the MR remains negative up to  $H=10 \text{ T}$ , which is different from Song *et al.*'s result,<sup>7</sup> showing the positive  $H^2$  dependence at high temperature. We must emphasize that the MR generally becomes significant at low temperature in most of the samples.

The temperature dependence of the zero-field resistivity is plotted in the inset of Fig. 2. The zero-field resistivity shows a negative  $d\rho/dT$  without a resistivity minimum between  $T$

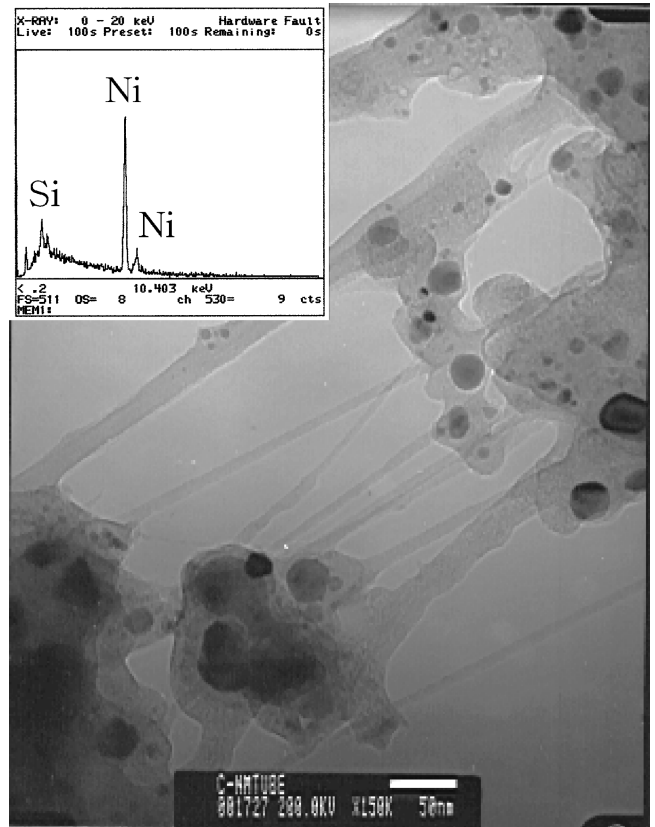


FIG. 1. TEM image of the SWCN bundles which contain nickel impurities. Inset: EDS show the sharp peaks originated from the nickel particles.

$=4.3$  and  $300 \text{ K}$ ,<sup>14</sup> and the room-temperature conductivity was  $\sigma_{RT} \approx 400 \text{ (S/cm)}$ . By heating the sample to  $T=370 \text{ K}$ , the positive  $d\rho/dT$  begins to appear at around  $T^*=320 \text{ K}$ . Thus the shallow resistance minimum temperature  $T^*$  is shifted to a higher temperature than those reported by Fischer *et al.*<sup>17</sup> The high  $T^*$  can be understood as due to the high intertubular couplings in the present sample. It is consistent with the recent studies on the pressure effects of transport of SWCN's by Fisher *et al.*,<sup>24</sup> who revealed the importance of the intertube ordering and attributed the inter-

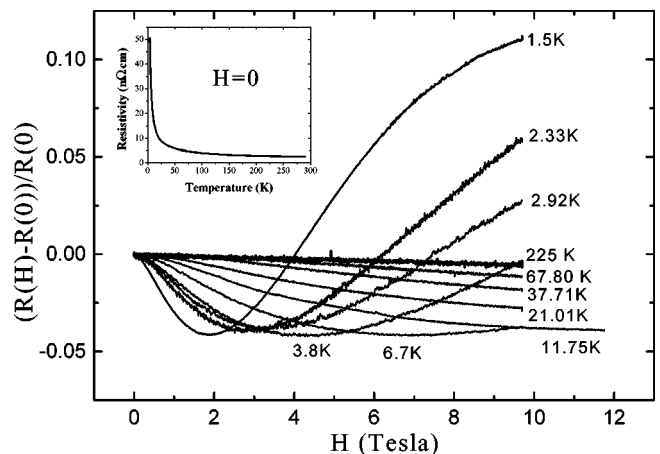


FIG. 2. MR of the SWCN network at  $T=1.5, 2.33, 2.92, 3.8,$   $6.7, 11.75, 21.01, 37.71, 67.80$  and  $225 \text{ K}$ . Inset: Temperature dependence of the zero-field resistivity between  $T=4.3$  and  $300 \text{ K}$ .

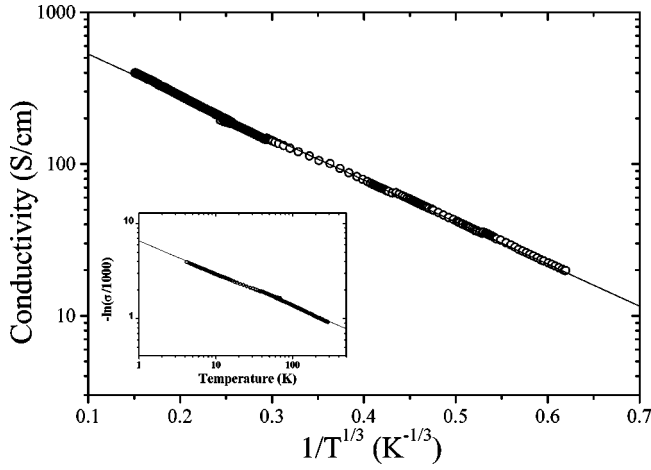


FIG. 3. Temperature dependence of the zero-field resistivity fitted to the two-dimensional variable range hopping formula.  $\sigma(T) = 1003.9 \exp[-(259.2/T)^{1/3}]$ . Inset: the slope gives the dimensional exponent  $d=1.922$ , indicating the two-dimensional VRH.

actions between the nanotubes to the crossover temperature  $T^*$ .

In view of the strong localization picture, we considered VRH-type conduction at first. The model fits our temperature dependence of the zero-field conductivity data very well as shown in Fig. 3. In Mott and Davis's VRH model,<sup>41</sup> the conductivity follows the formula  $\sigma(T) = \sigma_0 \exp[-(T_0/T)^{1/(d+1)}]$  ( $d$  is the dimension of the system). We have obtained the dimensional constant  $d=1.92$  by fitting  $\ln[-\ln(\sigma/1000)]$  versus  $\ln T$  as in the inset of Fig. 3, indicating that the two-dimensional VRH is dominant, and obtained  $T_0=259.2$  K. One might try to fit the observed negative MR data to the VRH theory of Fukuyama and Yoshida. Although the  $H^2$  dependence of MR at low field ( $H < 1$  T) can be explained under this scheme, the fitting results according to the theory of Ref. 42 of negative MR show the dimensionality parameter  $d=0.70$  which is not consistent with the result ( $d=1.92$ ) of the zero-field resistivity data fitting. One might argue that the reduction of dimensionality could occur due to the shrinkage of the wave func-

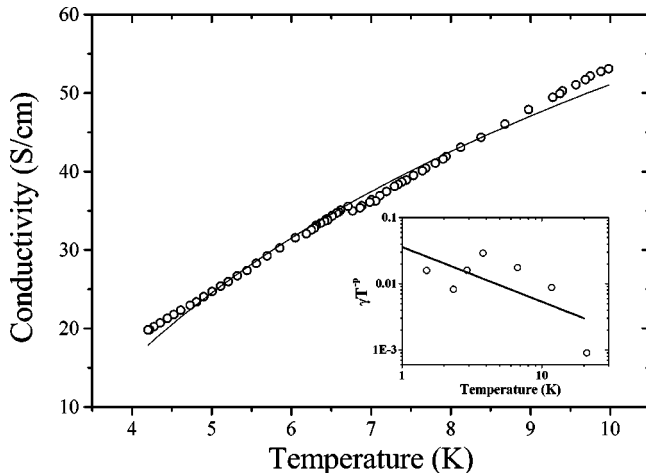


FIG. 4. Temperature dependence of the zero-field resistivity at low temperature fitted to the two-dimensional WL theory. Inset:  $p$  value fitting according to the two-dimensional WL ( $p=0.828$ ).

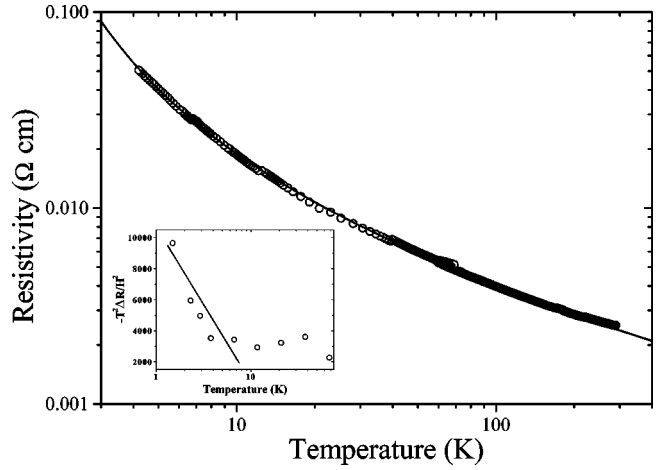


FIG. 5. Temperature dependence of the zero-field resistivity fitted to the Kondo equation. The left inset denotes the linear region between  $-T^2 \Delta R / H^2$  and  $\ln T$  below  $T < 10$  K.

tion under a magnetic field. However, since the fitting regime of the  $H^2$  dependence of MR is limited to the low magnetic field ( $H < 1$  T), the effect of the wave-function shrinkage is expected to be small. Therefore the negative MR cannot originate due to the strong localization effect (VRH).

Second, we tried to fit the zero-field conductivity with the WL theory at low temperatures ( $4.3 \text{ K} < T < 10 \text{ K}$ ) to see its suitability for our system.<sup>45</sup> In the WL theory, the characteristic length scale is the Thouless length  $L_{Th} \approx aT^{-p/2}$ . The value of  $p$  is determined by the temperature dependence of the scattering rate ( $\tau^{-1} \propto T^p$ ) from the dominant dephasing mechanism. We have tried to fit the data with the one- and two-dimensional WL formulas, as well as the three-dimensional WL formula. However, the one- and three-dimensional WL formulas do not fit both the zero-field resistance and the MR result together by the appropriate  $p$  values consistent with the theory. On the other hand, the two-dimensional WL formula [Eq. (1)] can fit the data reasonably well, as shown in Fig. 4:

$$\sigma(T) = \sigma(T_0) + \frac{e^2}{2\hbar\pi^2} \left[ \alpha p + \left( 1 - \frac{3}{4} \tilde{F}_\sigma \right) \right] \ln \left[ \frac{T}{T_0} \right]. \quad (1)$$

For an orbitally nondegenerate free-electron gas,  $\alpha=1$ , and  $p/2$  is the temperature index of the Thouless length  $L_{Th}$ . The Coulomb term is  $(1 - \frac{3}{4} \tilde{F}_\sigma)$ , where the size of the Hartree part  $\tilde{F}_\sigma$  depends on the screening length. The inset of Fig. 4 shows the fitting of the negative MR using the two-dimensional WL model of Eq. (2). The  $p$  value obtained by the fitting was  $p=0.828 \approx 1$ , which is consistent with the predicted value by the two-dimensional WL theory. This  $p$  value is similar to that of Song *et al.*,<sup>7</sup>

$$\Delta\sigma(H, T) = \frac{e^2}{2\pi^2\hbar} \left[ \psi \left[ \frac{1}{2} + \frac{1}{x} \right] + \ln(x) \right] \propto T^{-p} H \left( x = L_{Th}^2 \frac{4eH}{\hbar c} \ll 1, \quad L_{Th} \propto T^{-(p/2)} \right), \quad (2)$$

where  $\psi$  is the digamma function. The general behaviors in both the zero-field resistivity and the MR are indicative to those of the two-dimensional WL, although the estimated  $p$  value is slightly smaller than expected.

On the other hand, we have considered the effect of nickel impurities by fitting the data to the Kondo-effect formula as shown in Fig. 5. Kondo<sup>35</sup> suggested the contribution of extra  $s$ - $d$  exchange interaction to the temperature dependence of zero-field resistivity as following Eq. (3) for  $T > T_K$ :

$$\Delta\rho = \frac{3c}{\pi e^2 v_F^2 \hbar} \frac{\Omega}{N} \left\{ \sin^2 \eta - 2\pi^2 J^2 \rho_1^2 S(S+1) \cos^4 \eta \sin^2 \eta + \pi^2 J^2 \rho_1^2 S(S+1) \frac{\cos^4 \eta \cos 2\eta}{[1 - 2\tilde{J}\rho_1 \ln(T/D_\epsilon)]^2} \right\}. \quad (3)$$

$\eta$  is the phase shift due to the potential scattering given as  $\tan \eta = -\pi V \rho_1$ , where  $\rho_1$  is the carrier concentration per one spin degree of freedom near the Fermi energy, and  $V$  the magnitude of the potential energy.  $\Omega$  is the volume of the host metal,  $S$  the effective spin angular moment of unpaired spin in the existing magnetic impurities,  $D_\epsilon$  the cutoff energy which corresponds to the Fermi energy, and  $\tilde{J}$  the effective exchange interaction integral given as  $\tilde{J} = J \cos^2 \eta$ . The negative (positive)  $J$  value corresponds to the antiferromagnetic (ferromagnetic)  $s$ - $d$  exchange coupling between the conduction electrons and the localized moments. Because of the complexity of the equation, the fitting is not simple. The Origin 3.78 made by Microcal Software, Inc. was used to plot the data. The data fitting is done by the user-defined function program in the menu of the Origin 3.78. By repeating the numerical fitting in the menu with proper initial values, the errors between the fitted curve and the data could be reduced. The resultant fitting parameters are given in Table I. At extremely low temperature, there may be screening around the localized magnetic moment, which reduces the effective magnetic moment, reaching zero at  $T=0$ . The small magnetic moment ( $S=0.140$ ) may come from the screening around the nickel impurities. By a complete screening of the magnetic moment, the resistivity change will be gradually reduced as the temperature is lowered below the Kondo temperature ( $T < T_K$ ), following the Nagaoka's equation.<sup>34</sup> The Kondo temperature we have obtained is  $T_K = 1.03$  K, which is lower than the range of our measurement. Thus the condition  $T > T_K$  to use Eq. (3) is satisfied.

Negative magnetoresistance could originate due to the depression of the spin-flip scattering in the Kondo effect, which can be fitted to Eq. (4) (Ref. 36) at low magnetic field:

TABLE I. Fitting parameters of the temperature dependence of the resistivity obtained by the Kondo formula.

$\eta$	$J \rho_1$	$S$	$D_\epsilon$ (meV) <sup>a</sup>	$T_K$ (K)
$\pi/19.6$	$-0.618^b$	0.140	0.2	1.030 <sup>c</sup>

<sup>a</sup>Cutoff energy corresponding to the Fermi energy.

<sup>b</sup>The negative value refers to the antiferromagnetic coupling.

<sup>c</sup>Kondo temperature is given as  $T_K = (D/k_E) \exp(-1/2|J|\rho_1)$ .

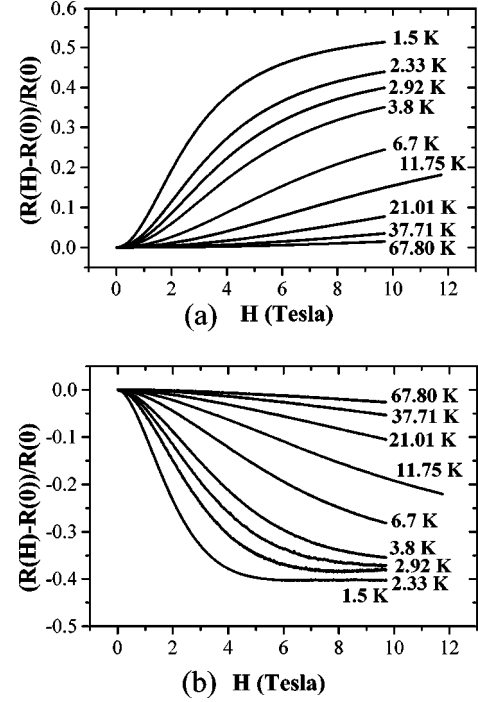


FIG. 6. (a) Calculated positive MR obtained by fitting the MR data of  $H > 7$  T to a Kamimura-type positive MR formula in two dimensions.  $a = 0.220$ ,  $b = 0.145$ , and  $T_0 = 259.2$  K. (b) The negative MR obtained by subtracting the calculated positive MR (a) from the experimental raw MR data.

$$\Delta\rho \approx -\frac{3\pi}{2\epsilon_F} \frac{m}{e^2 \hbar} \frac{c v_0}{9} \left( \frac{g \mu_B H}{k_B T} \right)^2 J^2 S(S+1) \times \left[ 1 + 4S(S+1) + \frac{3zJ}{\epsilon_F} \left[ 1 + 4S(S+1) \right] \ln \frac{k_B T}{2\epsilon_F} + 6.27S(S+1) + 1.11 \right] \left( \alpha = \frac{g \mu_B H}{k_B T} \ll 1 \right), \quad (4)$$

where  $v_0$  is the atomic volume of the host metal,  $c$  the impurity concentration, and  $z$  the number of conduction electrons per atom.

If  $-T^2$  is multiplied by Eq. (4), we can infer  $J^3 S \ln T$  dependence of  $-T^2 \Delta\rho / H^2$  ( $-T^2 \Delta\rho / H^2 \propto J^3 S \ln T$ ). At each temperature, we have fitted the  $H^2$  dependence of the low-field MR data to Eq. (4), and plotted  $-T^2 \Delta\rho / H^2$  versus  $\ln T$  in the inset of Fig. 5. The negative slope at  $T < 10$  K versus  $\ln T$  indicates that the exchange coupling is antiferromagnetic ( $J < 0$ ), which is consistent with the zero-field result. Regarding the Kondo effect, Gurgenshivili, Kharadze, and Nersesian calculated the MR in the case of large phase shift, which showed negative at low field and positive MR saturated at high field.<sup>39</sup> Although we tried to fit our MR data to this scheme, the phase shift turns out to be  $2\pi/7$  which is larger than  $\pi/4$ . Since the Kondo formula [Eqs. (3) and (4)] used to fit our data are based on the small phase shift ( $\eta \ll \pi/4$ ), the large phase shift and its sensitive change with the variation of parameters are difficult to understand. Therefore, the positive upturn of MR cannot be understood reasonably with the Kondo effect only.

To understand the positive upturn of MR at low temperature, we made the following two assumptions.<sup>9,44</sup> (i) The MR data are the sum of the positive and negative contributions,  $(\Delta\rho/\rho) = (\Delta\rho/\rho)_p + (\Delta\rho/\rho)_n$ . (ii) At high magnetic field, the positive contribution dominates the negative MR component which is saturated at this field. For the positive MR contribution, we use the magnetoconductance  $\Delta G/G$  of a Kamimura-type spin-dependent VRH contribution in two dimensions, as follows [Eq. (5)].<sup>9,43,44</sup>

$$\frac{\Delta G}{G} = -A_{KK} \frac{H^2}{H_{KK}^2 + H^2}, \quad \mu_B H_{KK} = a k_B T \left( \frac{T_0}{T} \right)^{1/3}, \quad (5)$$

$$A_{KK} = 1 - \exp \left[ -b \left( \frac{T_0}{T} \right)^{1/3} \right].$$

( $H_{KK}$  is the characteristic field for spin alignment,  $A_{KK}$  the saturation value of the magnetoconductance, and  $a$  and  $b$  are constants depending on the system.) Under assumption (ii), we fitted the data to Eq. (5) in the high-field regime ( $H > 7$  T). By fitting, we obtained  $a = 0.220$  and  $b = 0.145$ . The fitting curve for the positive MR is plotted in Fig. 6(a). Subtracting the positive contribution in Fig. 6(a) from the raw MR data shown in Fig. 2, the pure negative MR could be extracted as in Fig. 6(b). The overall behavior is monotonous without crosses and/or abrupt changes. With these schemes we can explain the positive upturn in MR data by adding (a) and (b) of Fig. 6. The positive MR may come from the two-dimensional spin-dependent VRH among the defects on the surface of tubes, and the negative MR might originate from the WL contribution. The negative contribution to the MR from the WL might be deformed by the extra spin exchange coupling with Ni particles.<sup>30</sup> It is not clear how large

the effect of Ni is. Interestingly, there were reports that WL may have difficulties in thin metal films containing magnetic impurities.<sup>30</sup> To understand the effect of magnetic impurities and the intrinsic conduction mechanism clearly, further experimental studies are ongoing.

#### IV. SUMMARY

We have measured the MR of a SWCN's network up to  $H = 10$  T as a function of temperature. The zero-field resistivity follows a two-dimensional VRH behavior well into the measured temperature range. The negative MR data can be fitted by the two-dimensional WL theory. The positive upturn of MR at low temperature seems to originate from Kamimura-type two-dimensional spin-dependent VRH. The inter tubular coupling could be important in our mat-type samples, leading to the high crossover temperature  $T^*$ , and the possible contribution from the magnetic impurity (Ni) introduced in synthesizing the SWCNs has been discussed.

#### ACKNOWLEDGMENTS

We would especially like to express our gratitude to Dr. J. H. Smet and Dr. A. Christian at MPI, Stuttgart, for allowing us to use their magnet system, and to Mee Jeong Kang at the Inter-University Center for Natural Science Research Facilities in Seoul National University for the elemental analysis using TEM and EDS. This work was jointly supported by the Korea Science and Engineering Foundation (KOSEF), Korea and the Deutsche Forschungsgemeinschaft (DFG), Germany. Partial support for G.T.K. was provided by the DAAD-KOSEF program and the European Community through the TMR contract NAMITECH.

\*Author to whom correspondence should be addressed. Electronic address: ywpark@plaza.snu.ac.kr

<sup>1</sup>S. Iijima, *Nature (London)* **354**, 56 (1991).

<sup>2</sup>N. Hamada, S. Sawada, and A. Oshiyama, *Phys. Rev. Lett.* **68**, 1579 (1992).

<sup>3</sup>L. Langer, L. Stockman, J. P. Heremans, V. Bayot, C. H. Olk, C. Van Haesendonck Y. Bruynseraede, and J.-P. Issi, *J. Mater. Res.* **9**, 927 (1994).

<sup>4</sup>J. Heremans, C. H. Olk, and D. T. Morelli, *Phys. Rev. B* **49**, 15122 (1994).

<sup>5</sup>A. P. Ramirez, R. C. Haddon, O. Zhou, R. M. Fleming, J. Jhang, S. M. McClure, and R. E. Smalley, *Science* **265**, 84 (1994).

<sup>6</sup>X. K. Wang, R. P. H. Chang, A. Patashinski, and J. B. Ketterson, *J. Mater. Res.* **9**, 1578 (1994).

<sup>7</sup>S. N. Song, X. K. Wang, R. P. H. Chang, and J. B. Ketterson, *Phys. Rev. Lett.* **72**, 697 (1994).

<sup>8</sup>M. F. Lin and K. W.-K. Shung, *Phys. Rev. B* **51**, 7592 (1995).

<sup>9</sup>A. Frydman and Z. Ovadyahu, *Solid State Commun.* **94**, 745 (1995).

<sup>10</sup>L. Langer, L. Stockman, J. P. Heremans, V. Bayot, C. H. Olk, C. Van Haesendonck, Y. Bruynseraede, and J.-P. Issi, *Synth. Met.* **70**, 1393 (1995).

<sup>11</sup>M. Kosaka, T. W. Ebbesen, H. Hiura, and K. Tanigaki, *Chem. Phys. Lett.* **233**, 47 (1995).

<sup>12</sup>L. Langer, V. Bayot, E. Grivei, J.-P. Issi, J. P. Heremans, C. H. Olk, L. Stockman, C. Van Haesendonck, and Y. Bruynseraede,

*Phys. Rev. Lett.* **76**, 479 (1996).

<sup>13</sup>N. H. March, J. A. Alonso, and A. Rubio, *Phys. Status Solidi B* **203**, 179 (1997).

<sup>14</sup>W. A. de Heer, W. S. Bacsá, A. Chatelain, T. Gerfin, R. Humphrey-Baker, L. Forro, and D. Ugarte, *Science* **268**, 845 (1995).

<sup>15</sup>T. W. Ebbesen, *Phys. Today* **49**(6), 26 (1996).

<sup>16</sup>S. J. Tans, M. H. Devoret, H. Dai, A. Thess, R. E. Smalley, L. J. Geerligs, and C. Dekker, *Nature (London)* **386**, 474 (1997).

<sup>17</sup>J. E. Fischer, H. Dai, A. Thess, R. Lee, N. M. Hanjani, D. L. Dehaas, and R. E. Smalley, *Phys. Rev. B* **55**, 4921 (1997).

<sup>18</sup>G. Baumgartner, M. Carrad, L. Zuppiroli, W. Bacsá, W. A. de Heer, and L. Forro, *Phys. Rev. B* **55**, 6704 (1997).

<sup>19</sup>C. Journet, W. K. Maser, P. Bernier, A. Loiseau, M. Lamydela Chapelle, S. Lefrant, P. Deniard, R. Lee, and J. E. Fischer, *Nature (London)* **388**, 756 (1997).

<sup>20</sup>A. B. Kaiser, G. Düsberg, and S. Roth, *Phys. Rev. B* **57**, 1418 (1998).

<sup>21</sup>G. S. Duesberg, M. Burghard, J. Muster, G. Philip, and S. Roth, *Chem. Commun. (Cambridge)* 435 (1998).

<sup>22</sup>J. Muster, M. Burghard, S. Roth, G. S. Duesberg, E. Hernandez, and A. Rubio, *J. Vac. Sci. Technol. B* **16**, 2796 (1998).

<sup>23</sup>J. Hone, I. Ellwood, M. Muno, A. Mizel, M. L. Cohen, A. Zettle, A. G. Rinzler, and R. E. Smalley, *Phys. Rev. Lett.* **80**, 1042 (1998).

- <sup>24</sup>J. E. Fischer, R. S. Lee, H. J. Kim, A. G. Rinzler, R. E. Smalley, S. L. Yaguzhinski, A. D. Bozhko, D. E. Sklovsky, and V. A. Nalimova, in *Proceedings of the Winter School on Carbon Nanotubes*, Kirchberg, Austria, March 1998, edited by H. Kuzmany *et al.* (Springer-Verlag, Berlin, in press).
- <sup>25</sup>P. Delaney, H. J. Choi, J. Ihm, S. G. Louie, and M. L. Cohen, *Nature (London)* **391**, 466 (1998).
- <sup>26</sup>T. W. Ebbesen, H. J. Lezec, H. Hiura, J. W. Bennett, H. F. Ghaemi, and T. Thio, *Nature (London)* **382**, 54 (1996).
- <sup>27</sup>Y. H. Lee, S. G. Kim, and D. Tamanek, *Phys. Rev. Lett.* **78**, 2393 (1997).
- <sup>28</sup>T. W. Odom, J.-L. Huang, P. Kim, and C. M. Lieber, *Nature (London)* **391**, 62 (1998).
- <sup>29</sup>J. W. G. Wildöer, L. C. Venema, A. G. Rinzler, R. E. Smalley, and C. Dekker, *Nature (London)* **391**, 59 (1998).
- <sup>30</sup>G. Li, M. Chen, G. Liu, M. Wang, S. Wang, and S. Yan, *Phys. Rev. B* **57**, 2683 (1998).
- <sup>31</sup>C. A. Domenicali and E. L. Christenson, *J. Appl. Phys.* **32**, 2450 (1961).
- <sup>32</sup>G. J. Van der Berg, in *Progress in Low Temperature Physics*, edited by C. J. Gorter (North-Holland, Amsterdam, 1964), Vol. IV, p. 194.
- <sup>33</sup>J. Kondo, *Prog. Theor. Phys.* **34**, 204 (1965).
- <sup>34</sup>Y. Nagaoka, *Phys. Rev.* **138**, A1112 (1965).
- <sup>35</sup>J. Kondo, *Phys. Rev.* **169**, 437 (1968).
- <sup>36</sup>M.-T. Beal-Monod and R. A. Weiner, *Phys. Rev.* **170**, 552 (1968).
- <sup>37</sup>M. D. Daybell and W. A. Steyert, *Rev. Mod. Phys.* **40**, 380 (1968).
- <sup>38</sup>R. More and H. Suhl, *Phys. Rev. Lett.* **20**, 500 (1968).
- <sup>39</sup>G. E. Gurgenshvili, G. A. Kharadze, and A. A. Nersesian, *J. Low Temp. Phys.* **1**, 633 (1969).
- <sup>40</sup>R. G. Sharma and M. S. R. Chari, *J. Low Temp. Phys.* **13**, 553 (1973).
- <sup>41</sup>N. F. Mott and E. A. Davis, *Electronic Processes in Non-Crystalline Materials*, 2nd ed. (Clarendon, Oxford, 1979), p. 30.
- <sup>42</sup>H. Fukuyama and K. Yoshida, *J. Phys. Soc. Jpn.* **46**, 102 (1979).
- <sup>43</sup>A. Kurobe and H. Kamimura, *J. Phys. Soc. Jpn.* **51**, 1904 (1982).
- <sup>44</sup>H. Kamimura, A. Kurobe, and T. Takemori, *Physica B&C* **117&118**, 652 (1983).
- <sup>45</sup>P. A. Lee and T. V. Ramakrishnan, *Rev. Mod. Phys.* **57**, 287 (1985).
- <sup>46</sup>V. Bayot, L. Piraux, J.-P. Michenaud, and J.-P. Issi, *Phys. Rev. B* **40**, 3514 (1989).